

## SPOOFING CYBER ATTACK DETECTION IN PROBE-BASED TRAFFIC MONITORING SYSTEMS USING MIXED INTEGER LINEAR PROGRAMMING

EDWARD S. CANEPA

King Abdullah University of Science and Technology  
Electrical Engineering Department  
Thuwal, Makkah 23955, KSA

ALEXANDRE M. BAYEN

University of California at Berkely  
Electrical Engineering and Computer Sciences  
Berkeley CA 94720-170, USA

CHRISTIAN G. CLAUDEL

King Abdullah University of Science and Technology  
Electrical Engineering Department  
Thuwal, Makkah 23955, KSA

**ABSTRACT.** Traffic sensing systems rely more and more on user generated (insecure) data, which can pose a security risk whenever the data is used for traffic flow control. In this article, we propose a new formulation for detecting malicious data injection in traffic flow monitoring systems by using the underlying traffic flow model. The state of traffic is modeled by the Lighthill-Whitham-Richards traffic flow model, which is a first order scalar conservation law with concave flux function. Given a set of traffic flow data generated by multiple sensors of different types, we show that the constraints resulting from this partial differential equation are mixed integer linear inequalities for a specific decision variable. We use this fact to pose the problem of detecting spoofing cyber attacks in probe-based traffic flow information systems as mixed integer linear feasibility problem. The resulting framework can be used to detect spoofing attacks in real time, or to evaluate the worst-case effects of an attack offline. A numerical implementation is performed on a cyber attack scenario involving experimental data from the *Mobile Century* experiment and the *Mobile Millennium* system currently operational in Northern California.

**1. Introduction.** The convergence of mobile sensing, communication and computing has led to the rise of a new class of systems known as *cyberphysical systems*, which are physical systems sensed and actuated by “cyber” agents, an example of which is the transportation network. Owing to their spatially and temporally distributed nature, such systems are often modeled as distributed parameter systems [23, 8, 19]. Estimating or controlling the state of a distributed parameter systems a very complex problem in general. It requires the integration of noisy

---

2010 *Mathematics Subject Classification.* 68U35, 90C11, 90C90.

*Key words and phrases.* Mixed integer linear programming, hyperbolic partial differential equations, cybersecurity.

measurement data with dynamical models, usually encoded by a *partial differential equation* (PDE). Incorporating the constraints encoded by the model into the estimation problem is difficult in general, since these constraints can be nonlinear, nonconvex, or even non-explicit. Ultimately, the model constraints can always be enforced through the use of *Monte Carlo* techniques, but these methods are challenging for large dimensional problems.

In transportation systems, a new form of sensing has emerged since a few years in the form of *probe vehicles*. In this paradigm, the vehicles themselves transmit their speed and location anonymously [26] to a central server, which uses this data in conjunction with fixed sensor data [27] to generate real-time traffic maps. While systems such as the *Mobile Millennium* system [26] have successfully demonstrated the concept, multiple issues remain in terms of security [1, 2]. Unlike fixed sensors which are difficult to tamper with, it is relatively easy for an attacker to generate fake data and inject it in the system to modify the estimates with dire consequences, in particular if the traffic estimates are used for optimal traffic control (traffic lights, ramp metering). Indeed, probe-based systems do not require strong authentication from the users to enhance user privacy [18].

Detecting such cyber attacks is a complex problem, since there is a wide range of possible traffic velocities and a great diversity of possible traffic patterns. Detecting fake data that follows some pattern (for instance if the faked data is periodic) or that falls out of physically reasonable bounds is easy. However, detecting fake data that is both random and consistent with a typical sensor measurement is difficult. In this situation, detecting fake data injection can only be done by checking the consistency of the data with respect to the model, which is assumed to hold perfectly (*i.e.* without model uncertainty) in the present article. Note that the interpretation of the results of this consistency check is complex: inconsistency may result from genuinely faulty sensors or even from local violations of the traffic flow model.

In the present article, we use the underlying traffic flow model, encoded by the *Lighthill-Whitham-Richards* (LWR) PDE to detect cyber attacks, assuming that data is generated by a set of fixed sensors and a set of probe vehicles. We show that the model-data consistency check problem can be posed as a *Mixed Integer Linear Program* (MILP). The importance of this formulation is significant, since it now provides an algorithmic solution method to this previously open problem, that could only be solved using Monte Carlo techniques or through approximations. We then illustrate these results by numerical implementations of the corresponding MILPs using real data from the *Mobile Century* experiment [17] and from the *Mobile Millennium* system [26].

The rest of this article is organized as follows. Section 2 defines the solution to the HJ PDE investigated in this article, as well as its properties. Section 3 formulates the initial, boundaries and internal conditions of the problem as a function of the input data. We then derive the structure of the HJ PDE model constraints in section 4, and pose the problem of detecting spoofing attacks as a Mixed Integer Linear feasibility problem. Section 5 shows how one can use this framework to detect a simulated spoofing attack on a real-life scenario, using experimental *Mobile Century* data, freely available from [26].

## 2. Model definition.

**2.1. Traffic-flow modeling using scalar Hamilton-Jacobi equations.** In the remainder of the article, we assume that the spatial domain representing the highway section is defined by  $[\xi, \chi]$ , where  $\xi$  and  $\chi$  respectively represent the upstream and downstream boundaries of the domain. We assume that the state of the system is described by a scalar function  $\mathbf{M}(\cdot, \cdot)$  of both time and space, known as *Moskowitz function* [21, 22]. The Moskowitz function is a possible macroscopic description of traffic flow, which appears linearly in the context of traffic. Let consecutive integer labels be assigned to vehicles entering the highway at location  $x = \xi$ . The Moskowitz function  $\mathbf{M}(\cdot, \cdot)$  is a continuous function satisfying  $\lfloor \mathbf{M}(t, x) \rfloor = n$  where  $n$  is the label of the vehicle located in  $x$  at time  $t$  [14, 15].

One of the most common models used to describe traffic flow is known as the *Lighthill-Whitham-Richards* (LWR) model. With this assumption, the Moskowitz function satisfies a *Hamilton-Jacobi* (HJ) PDE evolution equation:

$$\frac{\partial \mathbf{M}(t, x)}{\partial t} - \psi \left( -\frac{\partial \mathbf{M}(t, x)}{\partial x} \right) = 0 \quad (1)$$

The function  $\psi(\cdot)$  defined in equation (1) is the *Hamiltonian*. Several classes of weak solutions to equation (1) exist, such as viscosity solutions [12, 5] or Barron-Jensen/Frankowska (B-J/F) solutions [6, 16] used in the present article. The B-J/F solutions to equation (1) are fully characterized by a *Lax-Hopf* formula [4, 9], which was initially derived using the control framework of viability theory [3].

In the remainder of this article, we assume that the Hamiltonian is given by the following formula:

$$\psi(\rho) = \begin{cases} v_f \rho & : \rho \in [0, k_c] \\ w(\rho - \kappa) & : \rho \in [k_c, \kappa] \end{cases}$$

where

$$k_c = \frac{-w\kappa}{v_f - w}$$

Such Hamiltonian is often referred to in the transportation literature as *triangular fundamental diagram* [13, 15], and is commonly used to model traffic flow because of its robustness.

**2.2. Lax-Hopf formula for Hamilton-Jacobi equations.** In order to characterize the B-J/F solutions, we first need to define the Legendre-Fenchel transform of the Hamiltonian  $\psi(\cdot)$  as follows.

**Definition 2.1. [Legendre-Fenchel transform]** For a concave and upper semicontinuous Hamiltonian  $\psi(\cdot)$  defined as previously, the Legendre-Fenchel transform  $\varphi^*$  is given by:

$$\varphi^*(u) := \sup_{p \in \text{Dom}(\psi)} [p \cdot u + \psi(p)] \quad (2)$$

The inverse transform is defined [4] by:

$$\psi(p) := \inf_{u \in \text{Dom}(\varphi^*)} [\varphi^*(u) - p \cdot u] \quad (3)$$

Solving the HJ PDE (1) requires the definition of *value conditions*, which encode the traditional concepts of initial, boundary and internal conditions.

**Definition 2.2. [Value condition]** A value condition  $\mathbf{c}(\cdot, \cdot)$  is a lower semicontinuous function defined on a subset of  $[0, t_{\max}] \times [\xi, \chi]$ .

By convention, a value condition  $\mathbf{c}(\cdot, \cdot)$  as defined in Definition 2.2 satisfies  $\mathbf{c}(t, x) = +\infty$  if  $(t, x) \notin \text{Dom}(\mathbf{c})$ . The domain of definition of a value condition represents the subset of the space time domain  $\mathbb{R}_+ \times [\xi, \chi]$  in which we want the value condition to apply. For instance, imposing an upstream boundary condition  $\mathbf{c}_{\text{upstream}}(\cdot, \cdot)$  amounts to constraint the value of the state on the set  $\text{Dom}(\mathbf{c}_{\text{upstream}}) = \mathbb{R}_+ \times \{\xi\}$ .

In the remainder of this article, the solution  $\mathbf{M}_{\mathbf{c}}(\cdot, \cdot)$  to (1) associated with a value condition  $\mathbf{c}(\cdot, \cdot)$  is defined by the following Lax-Hopf formula [4, 9].

**Proposition 2.3. [Lax-Hopf formula]** *Let  $\psi(\cdot)$  be a concave and continuous Hamiltonian, let  $\varphi^*(\cdot)$  be the Legendre-Fenchel transform of  $\psi(\cdot)$  given by equation (2), and let  $\mathbf{c}(\cdot, \cdot)$  be a value condition, as in Definition 2.2. The B-J/F solution  $\mathbf{M}_{\mathbf{c}}(\cdot, \cdot)$  to (1) associated with  $\mathbf{c}(\cdot, \cdot)$  is defined [4, 9] algebraically by:*

$$\mathbf{M}_{\mathbf{c}}(t, x) = \inf_{(u, T) \in \text{Dom}(\varphi^*) \times \mathbb{R}_+} (\mathbf{c}(t - T, x + Tu) + T\varphi^*(u)) \quad (4)$$

Equation (4) implies the existence of a B-J/F solution  $\mathbf{M}_{\mathbf{c}}(\cdot, \cdot)$  for any value condition function  $\mathbf{c}(\cdot, \cdot)$ . However, the solution itself may be incompatible with the value condition that we imposed on it, *i.e.* we do not necessarily have  $\forall (t, x) \in \text{Dom}(\mathbf{c}), \mathbf{M}_{\mathbf{c}}(t, x) = \mathbf{c}(t, x)$ .

The structure of the Lax-Hopf formula (4), implies the following important property, known as *inf-morphism* property.

**Proposition 2.4. [Inf-morphism property]** *Let the value condition  $\mathbf{c}(\cdot, \cdot)$  be minimum of a finite number of lower semicontinuous functions:*

$$\forall (t, x) \in [0, t_{\max}] \times [\xi, \chi], \quad \mathbf{c}(t, x) := \min_{j \in J} \mathbf{c}_j(t, x) \quad (5)$$

*The solution  $\mathbf{M}_{\mathbf{c}}(\cdot, \cdot)$  associated with the above value condition can be decomposed [4, 9, 10] as:*

$$\forall (t, x) \in [0, t_{\max}] \times [\xi, \chi], \quad \mathbf{M}_{\mathbf{c}}(t, x) = \min_{j \in J} \mathbf{M}_{\mathbf{c}_j}(t, x) \quad (6)$$

**2.3. Model constraints.** In the remainder of this article, we decompose the value condition  $\mathbf{c}(\cdot, \cdot)$  into block value conditions  $\mathbf{c}_j$ ,  $j \in J$  each representing some measurement data. The relation between block value conditions and measurement data is presented in section 3. The inf-morphism property and Lax-Hopf formula (4) imply the following compatibility property:

**Proposition 2.5. [Model compatibility of block value conditions]** *Let  $\mathbf{c}(\cdot, \cdot) = \min_{j \in J} \mathbf{c}_j(\cdot, \cdot)$  be given, and let  $\mathbf{M}_{\mathbf{c}}(\cdot, \cdot)$  be defined as in (4). The value condition  $\mathbf{c}(\cdot, \cdot)$  satisfies  $\forall (t, x) \in \text{Dom}(\mathbf{c}), \mathbf{M}_{\mathbf{c}}(t, x) = \mathbf{c}(t, x)$  if and only if the following inequality constraints are satisfied:*

$$\mathbf{M}_{\mathbf{c}_j}(t, x) \geq \mathbf{c}_i(t, x) \quad \forall (t, x) \in \text{Dom}(\mathbf{c}_i), \quad \forall (i, j) \in J^2 \quad (7)$$

The proof of this proposition is available in [11].

When the above compatibility property is satisfied, all value conditions can be imposed in the strong sense [24], *i.e.* the solution to the HJ PDE (1) will be identical to the value conditions on their respective domains of definition.

In addition to the above proposition, the Moskowitz function  $\mathbf{M}_{\mathbf{c}}(\cdot, \cdot)$  has to be continuous by construction [22, 7], which yields additional compatibility conditions. We outline these compatibility conditions in Section 4

**3. Explicit solutions to piecewise affine initial, boundary and internal conditions.** Multiple types of value conditions can be incorporated into the estimation problem. In the present article, we include initial, boundary and internal conditions. The initial and boundary conditions are typically measured (with some error) using fixed sensors, such as inductive loop detectors, magnetometers or traffic cameras. Note that an increasing proportion of traffic data is generated by mobile sensors onboard vehicles, also referred to as *probe data* [25], which generate *internal conditions* [9].

**3.1. Definition of affine initial, boundary and internal conditions.** The formal definition of initial, boundary (upstream, downstream) and internal conditions associated with the HJ PDE (1) is the subject of the following definition.

**Definition 3.1. [Affine initial, boundary and internal conditions]** Let us define  $\mathbb{K} = \{0, \dots, k_{\max}\}$ ,  $\mathbb{N} = \{0, \dots, n_{\max}\}$  and  $\mathbb{M} = \{0, \dots, m_{\max}\}$ . For all  $k \in \mathbb{K}$ ,  $n \in \mathbb{N}$  and  $m \in \mathbb{M}$ , we define the following functions, respectively called initial (uniformly spaced in position by  $X$ ), upstream, downstream (uniformly spaced in time by  $T$ ) and internal conditions:

$$M_k(t, x) = \begin{cases} -\sum_{i=0}^{k-1} \rho(i)X \\ -\rho(k)(x - kX) \\ +\infty \end{cases} \begin{cases} \text{if } t = 0 \\ \text{and } x \in [kX, (k+1)X] \\ \text{otherwise} \end{cases} \quad (8)$$

$$\gamma_n(t, x) = \begin{cases} \sum_{i=0}^{n-1} q_{\text{in}}(i)T \\ +q_{\text{in}}(n)(t - nT) \\ +\infty \end{cases} \begin{cases} \text{if } x = \xi \\ \text{and } t \in [nT, (n+1)T] \\ \text{otherwise} \end{cases} \quad (9)$$

$$\beta_n(t, x) = \begin{cases} \sum_{i=0}^{n-1} q_{\text{out}}(i)T \\ +q_{\text{out}}(n)(t - nT) \\ -\sum_{k=0}^{k_{\max}} \rho(k)X \\ +\infty \end{cases} \begin{cases} \text{if } x = \chi \\ \text{and } t \in [nT, (n+1)T] \\ \text{otherwise} \end{cases} \quad (10)$$

$$\mu_m(t, x) = \begin{cases} L_m + r_m(t - t_{\min}(m)) \\ +v^{\text{meas}}(m)(t - t_{\min}(m)) \\ +\infty \end{cases} \begin{cases} \text{if } x = x_{\min}(m) \\ \text{and } t \in [t_{\min}(m), t_{\max}(m)] \\ \text{otherwise} \end{cases} \quad (11)$$

where  $v^{\text{meas}}(m) = \frac{x_{\max}(m) - x_{\min}(m)}{t_{\max}(m) - t_{\min}(m)}$

The affine initial, upstream, downstream and internal conditions defined above for the HJ PDE (1) are equivalent to constant initial, upstream and downstream boundary conditions for the LWR PDE [20]. The domains of definition of these functions are illustrated in Figure 1.

Note that for real-life problems, the initial, boundary and internal conditions are not known exactly, which we will assume to be the case in the remainder of this article. In particular, we do not know the exact values of the initial densities  $\rho(\cdot)$ , the boundary flows  $q_{\text{in}}(\cdot)$  and  $q_{\text{out}}(\cdot)$ , as well as the coefficients  $L_m$  and  $r_m$  of the internal conditions. Some coefficients such as  $q_{\text{in}}(\cdot)$  and  $q_{\text{out}}(\cdot)$  can be measured with some uncertainty, but some other coefficients such as  $L_m$  and  $r_m$  cannot be measured experimentally. These variables will act as part of our decision variable for the Mixed Integer Linear Program (MILP) derived in Section 4.

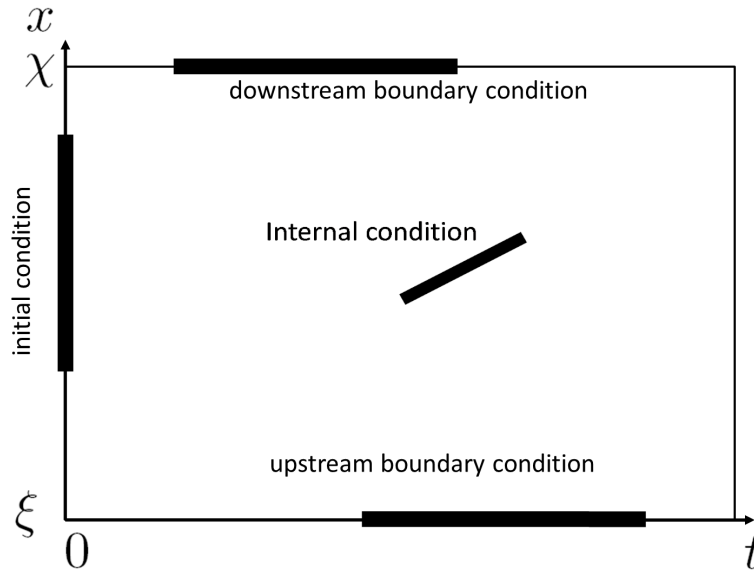


FIGURE 1. **Domains of the initial, upstream, downstream and internal boundary conditions.** The block upstream and downstream boundary conditions respectively denoted by  $\gamma_n(\cdot, \cdot)$  and  $\beta_n(\cdot, \cdot)$  are defined on line segments corresponding to the upstream and downstream boundaries of the physical domain. In contrast, the block initial conditions  $M_k(\cdot, \cdot)$  are defined on line segments corresponding to the initial time. The internal conditions  $\mu_m(\cdot, \cdot)$  are defined on line segments inside the computational domain. Note that the actual problem involves block initial conditions covering the entire physical domain  $[\xi, \chi]$ , and block boundary conditions covering the temporal domain  $[0, t_{\max}]$ , but that these functions are unknown (or only partially known).

**3.2. Analytical solutions to affine initial, boundary and internal conditions.** Given the affine initial, upstream, downstream and internal conditions defined above, the corresponding solutions  $\mathbf{M}_{M_k}(\cdot, \cdot)$ ,  $\mathbf{M}_{\gamma_n}(\cdot, \cdot)$ ,  $\mathbf{M}_{\beta_n}(\cdot, \cdot)$  and  $\mathbf{M}_{\mu_m}(\cdot, \cdot)$  defined by the Lax-Hopf formula (4) can be computed explicitly [11, 20] as closed-form expressions, which correspond to equations (13), (12), (14) and (15) below.

$$\mathbf{M}_{\gamma_n}(t, x) = \begin{cases} +\infty & \text{if } t \leq nT + \frac{x-\xi}{v} \\ \sum_{i=0}^{n-1} q_{\text{in}}(i)T & \\ +q_{\text{in}}(n)(t - \frac{x-\xi}{v} - nT) & \text{if } nT + \frac{x-\xi}{v} \leq t \\ & \text{and } t \leq (n+1)T \\ & + \frac{x-\xi}{v} \\ \sum_{i=0}^n q_{\text{in}}(i)T & \\ +\rho_c v(t - (n+1)T - \frac{x-\xi}{v}) & \text{otherwise} \end{cases} \tag{12}$$

$$\mathbf{M}_{M_k}(t, x) = \begin{cases} +\infty & \text{if } x \leq kX + wt \\ & \text{or } x \geq (k+1)X + vt \\ -\sum_{i=0}^{k-1} \rho(i)X \\ +\rho(k)(tv + kX - x) & \text{if } kX + tv \leq x \\ & \text{and } (k+1)X + tv \geq x \\ & \text{and } \rho(k) \leq \rho_c \\ -\sum_{i=0}^{k-1} \rho(i)X \\ +\rho_c(tv + kX - x) & \text{if } kX + tv \geq x \\ & \text{and } kX + tv \leq x \\ & \text{and } \rho(k) \leq \rho_c \\ -\sum_{i=0}^{k-1} \rho(i)X \\ +\rho(k)(tw + kX - x) \\ -\rho_m tw & \text{if } kX + tw \leq x \\ & \text{and } (k+1)X + tw \geq x \\ & \text{and } \rho(k) \geq \rho_c \\ -\sum_{i=0}^k \rho(i)X \\ \rho_c(tw + (k+1)X - x) \\ -\rho_m tw & \text{if } (k+1)X + tv \geq x \\ & \text{and } (k+1)X + tw \leq x \\ & \text{and } \rho(k) \geq \rho_c \end{cases} \quad (13)$$

$$\mathbf{M}_{\beta_n}(t, x) = \begin{cases} +\infty & \text{if } t \leq nT \\ & +\frac{x-\chi}{w} \\ -\sum_{k=0}^{k_{max}} \rho(k)X + \sum_{i=0}^{n-1} q_{out}(i)T \\ +q_{out}(n)(t - \frac{x-\chi}{w} - nT) \\ -\rho_m(x - \chi) & \text{if } nT \\ & +\frac{x-\chi}{w} \leq t \\ & \text{and } t \leq (n+1)T \\ & +\frac{x-\chi}{w} \\ -\sum_{k=0}^{k_{max}} \rho(k)X + \sum_{i=0}^n q_{out}(i)T \\ +\rho_c v(t - (n+1)T - \frac{x-\chi}{v}) & \text{otherwise} \end{cases} \quad (14)$$

$$\mathbf{M}_{\mu_m}(t, x) = \begin{cases} L_m + \\ r_m \left( t - \frac{x - x_{\min}(m) - v \frac{\text{meas}(m)(t - t_{\min}(m))}{w - v \text{meas}(m)}}{w - v \text{meas}(m)} - t_{\min}(m) \right) \\ \text{if } x \geq x_{\min}(m) + v \text{meas}(m)(t - t_{\min}(m)) \\ \text{and } x \geq x_{\max}(m) + v(t - t_{\max}(m)) \\ \text{and } x \leq x_{\min}(m) + v(t - t_{\min}(m)) \\ L_m + \\ r_m \left( t - \frac{x - x_{\min}(m) - v \frac{\text{meas}(m)(t - t_{\min}(m))}{w - v \text{meas}(m)}}{w - v \text{meas}(m)} - t_{\min}(m) \right) \\ +k_c(v - w) \frac{x - x_{\min}(m) - v \frac{\text{meas}(m)(t - t_{\min}(m))}{w - v \text{meas}(m)}}{w - v \text{meas}(m)} \\ \text{if } x \leq x_{\min}(m) + v \text{meas}(m)(t - t_{\min}(m)) \\ \text{and } x \leq x_{\max}(m) + w(t - t_{\max}(m)) \\ \text{and } x \geq x_{\min}(m) + w(t - t_{\min}(m)) \\ L_m + r_m(t_{\max}(m) - t_{\min}(m)) + \\ (t - t_{\max}(m))k_c \left( v - \frac{x - x_{\max}(m)}{t - t_{\max}(m)} \right) \\ \text{if } x \leq x_{\max}(m) + v(t - t_{\max}(m)) \\ \text{and } x \geq x_{\max}(m) + w(t - t_{\max}(m)) \\ +\infty \text{ otherwise} \end{cases} \quad (15)$$

The closed-form expressions of  $\mathbf{M}_{M_k}(\cdot, \cdot)$ ,  $\mathbf{M}_{\gamma_n}(\cdot, \cdot)$ ,  $\mathbf{M}_{\beta_n}(\cdot, \cdot)$  and  $\mathbf{M}_{\mu_m}(\cdot, \cdot)$  are very important: they enable one to compute the solution to the HJ PDE (1) semi-analytically for a very low computational cost using the inf-morphism property [9, 20]. They also enable one to write the model compatibility constraint condition (7) as a set of linear inequalities in a specific decision variable.

**4. Derivation of the spoofing attack detection scheme as Mixed-Integer-Linear-Programming.** As outlined earlier, deriving the constraints of an HJ PDE on initial/boundary/internal condition coefficients is complex in general, as the constraints may not be explicit. In the present case, our objective is to verify that a set of initial, boundary and internal conditions can be found such that the model applies in the strong sense. These constraints, known as *model constraints* define a set of allowable coefficients of the initial, boundary and internal conditions for which the model applies in the strong sense.

In addition to these model constraints, the value of the coefficients of the initial/boundary/internal conditions is also constrained by the data. These data constraints are translating the fact that the actual value of these coefficients is within some bounds that are a function of the observed data and of the sensor performance characteristics. We present an example of such data constraints later in the article.

**4.1. Model constraints.** We now instantiate the model constraints using the explicit solutions defined above as well as the inf-morphism property.

**Proposition 4.1.** [*Model constraints*] *The model constraints (7) can be expressed as the following finite set of convex inequality constraints:*

$$\left\{ \begin{array}{ll} \mathbf{M}_{M_k}(0, pX) \geq M_p(0, pX) & \forall (k, p) \in \mathbb{K}^2 \\ \mathbf{M}_{M_k}(pT, \chi) \geq \beta_p(pT, \chi) & \forall k \in \mathbb{K}, \forall p \in \mathbb{N} \\ \mathbf{M}_{M_k}\left(\frac{\chi - x_{k+1}}{v}, \chi\right) \geq & \\ \beta_p\left(\frac{\chi - x_{k+1}}{v}, \chi\right) & \forall k \in \mathbb{K}, \forall p \in \mathbb{N} \text{ s. t.} \\ & \frac{\chi - x_{k+1}}{v} \in [pT, \\ & (p+1)T] \\ \mathbf{M}_{M_k}(pT, \xi) \geq \gamma_p(pT, \xi) & \forall k \in \mathbb{K}, \forall p \in \mathbb{N} \\ \mathbf{M}_{M_k}\left(\frac{\xi - x_k}{w}, \xi\right) \geq \gamma_p\left(\frac{\xi - x_k}{w}, \xi\right) & \forall k \in \mathbb{K}, \forall p \in \mathbb{N} \text{ s. t.} \\ & \frac{\xi - x_k}{w} \in [pT, (p+1)T] \end{array} \right. \quad (16)$$

$$\left\{ \begin{array}{l} \mathbf{M}_{M_k}(t_{\min}(m), x_{\min}(m)) \geq \mu_m(t_{\min}(m), x_{\min}(m)) \\ \quad \forall k \in \mathbb{K}, \forall m \in \mathbb{M} \\ \mathbf{M}_{M_k}(t_{\max}(m), x_{\max}(m)) \geq \mu_m(t_{\max}(m), x_{\max}(m)) \\ \quad \forall k \in \mathbb{K}, \forall m \in \mathbb{M} \\ \mathbf{M}_{M_k}(t_1(m, k), x_1(m, k)) \geq \mu_m(t_1(m, k), x_1(m, k)) \\ \quad \forall k \in \mathbb{K}, \forall m \in \mathbb{M} \text{ s. t. } t_1(m, k) \in [t_{\min}(m); t_{\max}(m)] \\ \mathbf{M}_{M_k}(t_2(m, k), x_2(m, k)) \geq \mu_m(t_2(m, k), x_2(m, k)) \\ \quad \forall k \in \mathbb{K}, \forall m \in \mathbb{M} \text{ s. t. } t_2(m, k) \in [t_{\min}(m); t_{\max}(m)] \\ \mathbf{M}_{M_k}(t_3(m, k), x_3(m, k)) \geq \mu_m(t_3(m, k), x_3(m, k)) \\ \quad \forall k \in \mathbb{K}, \forall m \in \mathbb{M} \text{ s. t. } t_3(m, k) \in [t_{\min}(m); t_{\max}(m)] \\ \mathbf{M}_{M_k}(t_4(m, k), x_4(m, k)) \geq \mu_m(t_4(m, k), x_4(m, k)) \\ \quad \forall k \in \mathbb{K}, \forall m \in \mathbb{M} \text{ s. t. } t_4(m, k) \in [t_{\min}(m); t_{\max}(m)] \end{array} \right. \quad (17)$$

$$\left\{ \begin{array}{ll} \mathbf{M}_{\gamma_n}(pT, \xi) \geq \gamma_p(pT, \xi) & \forall (n, p) \in \mathbb{N}^2 \\ \mathbf{M}_{\gamma_n}(pT, \chi) \geq \beta_p(pT, \chi) & \forall (n, p) \in \mathbb{N}^2 \\ \mathbf{M}_{\gamma_n}(nT + \frac{\chi - \xi}{v}, \chi) \geq \beta_p(nT + \frac{\chi - \xi}{v}, \chi) & \forall (n, p) \in \mathbb{N}^2 \text{ s. t. } nT + \frac{\chi - \xi}{v} \in [pT, (p+1)T] \end{array} \right. \quad (18)$$

$$\left\{ \begin{array}{ll} \mathbf{M}_{\gamma_n}(t_{\min}(m), x_{\min}(m)) \geq \mu_m(t_{\min}(m), x_{\min}(m)) & \forall n \in \mathbb{N}, \forall m \in \mathbb{M} \\ \mathbf{M}_{\gamma_n}(t_{\max}(m), x_{\max}(m)) \geq \mu_m(t_{\max}(m), x_{\max}(m)) & \forall n \in \mathbb{N}, \forall m \in \mathbb{M} \\ \mathbf{M}_{\gamma_n}(t_5(m, n), x_5(m, n)) \geq \mu_m(t_5(m, n), x_5(m, n)) & \forall n \in \mathbb{N}, \forall m \in \mathbb{M} \text{ s. t. } t_5(m, n) \in [t_{\min}(m); t_{\max}(m)] \end{array} \right. \quad (19)$$

$$\left\{ \begin{array}{ll} \mathbf{M}_{\beta_n}(pT, \xi) \geq \gamma_p(pT, \xi) & \forall (n, p) \in \mathbb{N}^2 \\ \mathbf{M}_{\beta_n}(nT + \frac{\xi - \chi}{w}, \xi) \geq \gamma_p(nT + \frac{\xi - \chi}{w}, \xi) & \forall (n, p) \in \mathbb{N}^2 \text{ s. t. } nT + \frac{\xi - \chi}{w} \in [pT, (p+1)T] \\ \mathbf{M}_{\beta_n}(pT, \chi) \geq \beta_p(pT, \chi) & \forall (n, p) \in \mathbb{N}^2 \end{array} \right. \quad (20)$$

$$\left\{ \begin{array}{ll} \mathbf{M}_{\beta_n}(t_{\min}(m), x_{\min}(m)) \geq \mu_m(t_{\min}(m), x_{\min}(m)) & \forall n \in \mathbb{N}, \forall m \in \mathbb{M} \\ \mathbf{M}_{\beta_n}(t_{\max}(m), x_{\max}(m)) \geq \mu_m(t_{\max}(m), x_{\max}(m)) & \forall n \in \mathbb{N}, \forall m \in \mathbb{M} \\ \mathbf{M}_{\beta_n}(t_6(m, n), x_6(m, n)) \geq \mu_m(t_6(m, n), x_6(m, n)) & \forall n \in \mathbb{N}, \forall m \in \mathbb{M} \text{ s. t. } t_6(m, n) \in [t_{\min}(m); t_{\max}(m)] \end{array} \right. \quad (21)$$

$$\left\{ \begin{array}{ll} \mathbf{M}_{\mu_m}(pT, \xi) \geq \gamma_p(pT, \xi) & \forall (m, p) \in \mathbb{M} \times \mathbb{N} \quad (vii)(a) \\ \mathbf{M}_{\mu_m}(t_7(m), \xi) \geq \gamma_p(t_7(m), \xi) & \forall (m, p) \in \mathbb{M} \times \mathbb{N} \text{ s. t. } t_7(m) \in [pT, (p+1)T] \quad (vii)(b) \\ \mathbf{M}_{\mu_m}(t_8(m), \xi) \geq \gamma_p(t_8(m), \xi) & \forall (m, p) \in \mathbb{M} \times \mathbb{N} \text{ s. t. } t_8(m) \in [pT, (p+1)T] \quad (vii)(c) \end{array} \right. \quad (22)$$

$$\left\{ \begin{array}{ll} \mathbf{M}_{\mu_m}(pT, \chi) \geq \beta_p(pT, \chi) & \forall (m, p) \in \mathbb{M} \times \mathbb{N} \quad (viii)(a) \\ \mathbf{M}_{\mu_m}(t_9(m), \chi) \geq \beta_p(t_9(m), \chi) & \forall (m, p) \in \mathbb{M} \times \mathbb{N} \text{ s. t. } t_9(m) \in [pT, (p+1)T] \quad (viii)(b) \\ \mathbf{M}_{\mu_m}(t_{10}(m), \chi) \geq \beta_p(t_{10}(m), \chi) & \forall (m, p) \in \mathbb{M} \times \mathbb{N} \text{ s. t. } t_{10}(m) \in [pT, (p+1)T] \quad (viii)(c) \end{array} \right. \quad (23)$$

$$\left\{ \begin{array}{ll} \mathbf{M}_{\mu_m}(t_{\min}(p), x_{\min}(p)) \geq \mu_p(t_{\min}(p), x_{\min}(p)) & \forall (m, p) \in \mathbb{M}^2 \quad (ix)(a) \\ \mathbf{M}_{\mu_m}(t_{\min}(p), x_{\max}(p)) \geq \mu_p(t_{\min}(p), x_{\max}(p)) & \forall (m, p) \in \mathbb{M}^2 \quad (ix)(b) \\ \mathbf{M}_{\mu_m}(t_{11}(m, p), x_{11}(m, p)) \geq \mu_p(t_{11}(m, p), x_{11}(m, p)) & \forall (m, p) \in \mathbb{M}^2 \text{ s. t. } t_{11}(m, p) \in [t_{\min}(p), t_{\max}(p)] \quad (ix)(c) \\ \mathbf{M}_{\mu_m}(t_{12}(m, p), x_{12}(m, p)) \geq \mu_p(t_{12}(m, p), x_{12}(m, p)) & \forall (m, p) \in \mathbb{M}^2 \text{ s. t. } t_{12}(m, p) \in [t_{\min}(p), t_{\max}(p)] \quad (ix)(d) \\ \mathbf{M}_{\mu_m}(t_{13}(m, p), x_{13}(m, p)) \geq \mu_p(t_{13}(m, p), x_{13}(m, p)) & \forall (m, p) \in \mathbb{M}^2 \text{ s. t. } t_{13}(m, p) \in [t_{\min}(p), t_{\max}(p)] \quad (ix)(e) \\ \mathbf{M}_{\mu_m}(t_{14}(m, p), x_{14}(m, p)) \geq \mu_p(t_{14}(m, p), x_{14}(m, p)) & \forall (m, p) \in \mathbb{M}^2 \text{ s. t. } t_{14}(m, p) \in [t_{\min}(p), t_{\max}(p)] \quad (ix)(f) \\ \mathbf{M}_{\mu_m}(t_{15}(m, p), x_{15}(m, p)) \geq \mu_p(t_{15}(m, p), x_{15}(m, p)) & \forall (m, p) \in \mathbb{M}^2 \text{ s. t. } t_{15}(m, p) \in [t_{\min}(p), t_{\max}(p)] \quad (ix)(g) \end{array} \right. \quad (24)$$

where the coefficients  $t_1(m, k)$ ,  $x_1(m, k)$ ,  $t_2(m, k)$ ,  $x_2(m, k)$ ,  $t_3(m, k)$ ,  $x_3(m, k)$ ,  $t_4(m, k)$ ,  $x_4(m, k)$ ,  $t_5(m, n)$ ,  $x_5(m, n)$ ,  $t_6(m, n)$ ,  $x_6(m, n)$ ,  $t_7(m)$ ,  $t_8(m)$ ,  $t_9(m)$ ,  $t_{10}(m)$ ,  $t_{11}(m, p)$ ,  $x_{11}(m, p)$ ,  $t_{12}(m, p)$ ,  $x_{12}(m, p)$ ,  $t_{13}(m, p)$ ,  $x_{13}(m, p)$ ,  $t_{14}(m, p)$ ,  $x_{14}(m, p)$ ,  $t_{15}(m, p)$  and  $x_{15}(m, p)$  are given by equations (25), (26) and (27) below:

$$\left\{ \begin{array}{l} t_1(m, k) = \frac{x_{\min}(m) - (k+1)X - v^{\text{meas}}(m)t_{\min}(m)}{v - v^{\text{meas}}(m)} \\ x_1(m, k) = x_{\min}(m) + \\ v^{\text{meas}}(m) \left( \frac{x_{\min}(m) - (k+1)X - v^{\text{meas}}(m)t_{\min}(m)}{v - v^{\text{meas}}(m)} - t_{\min}(m) \right) \\ t_2(m, k) = \frac{x_{\min}(m) - kX - v^{\text{meas}}(m)t_{\min}(m)}{w - v^{\text{meas}}(m)} \\ x_2(m, k) = x_{\min}(m) + \\ v^{\text{meas}}(m) \left( \frac{x_{\min}(m) - kX - v^{\text{meas}}(m)t_{\min}(m)}{w - v^{\text{meas}}(m)} - t_{\min}(m) \right) \\ t_3(m, k) = \frac{x_{\min}(m) - kX - v^{\text{meas}}(m)t_{\min}(m)}{v - v^{\text{meas}}(m)} \\ x_3(m, k) = x_{\min}(m) + \\ v^{\text{meas}}(m) \left( \frac{x_{\min}(m) - kX - v^{\text{meas}}(m)t_{\min}(m)}{v - v^{\text{meas}}(m)} - t_{\min}(m) \right) \\ t_4(m, k) = \frac{x_{\min}(m) - (k+1)X - v^{\text{meas}}(m)t_{\min}(m)}{w - v^{\text{meas}}(m)} \\ x_4(m, k) = x_{\min}(m) + \\ v^{\text{meas}}(m) \left( \frac{x_{\min}(m) - (k+1)X - v^{\text{meas}}(m)t_{\min}(m)}{w - v^{\text{meas}}(m)} - t_{\min}(m) \right) \end{array} \right. \quad (25)$$

$$\left\{ \begin{array}{l} t_5(m, n) = \frac{nTv - v^{\text{meas}}(m)t_{\min}(m) + x_{\min}(m) - \xi}{v - v^{\text{meas}}(m)} \\ x_5(m, n) = x_{\min}(m) + \\ v^{\text{meas}}(m) \left( \frac{nTv - v^{\text{meas}}(m)t_{\min}(m) + x_{\min}(m) - \xi}{v - v^{\text{meas}}(m)} - t_{\min}(m) \right) \\ t_6(m, n) = \frac{nTw - v^{\text{meas}}(m)t_{\min}(m) + x_{\min}(m) - \chi}{w - v^{\text{meas}}(m)} \\ x_6(m, n) = x_{\min}(m) + \\ v^{\text{meas}}(m) \left( \frac{nTw - v^{\text{meas}}(m)t_{\min}(m) + x_{\min}(m) - \chi}{w - v^{\text{meas}}(m)} - t_{\min}(m) \right) \\ t_7(m) = \frac{\xi - x_{\min}(m) + wt_{\min}(m)}{v} \\ t_8(m) = \frac{\xi - x_{\max}(m) + wt_{\max}(m)}{v} \\ t_9(m) = \frac{\chi - x_{\min}(m) + vt_{\min}(m)}{v} \\ t_{10}(m) = \frac{\chi - x_{\max}(m) + vt_{\max}(m)}{v} \end{array} \right. \quad (26)$$

and

$$\left\{ \begin{array}{l} t_{11}(m, p) = \frac{x_{\min}(m) - x_{\min}(p) + v^{\text{meas}}(p)t_{\min}(p) - v^{\text{meas}}(m)t_{\min}(m)}{v^{\text{meas}}(p) - v^{\text{meas}}(m)} \\ x_{11}(m, p) = x_{\min}(p) + v^{\text{meas}}(p) \left( -t_{\min}(p) + \right. \\ \left. \frac{x_{\min}(m) - x_{\min}(p) + v^{\text{meas}}(p)t_{\min}(p) - v^{\text{meas}}(m)t_{\min}(m)}{v^{\text{meas}}(p) - v^{\text{meas}}(m)} \right) \\ t_{12}(m, p) = \frac{x_{\max}(m) - x_{\min}(p) + v^{\text{meas}}(p)t_{\min}(p) - vt_{\max}(m)}{v^{\text{meas}}(p) - v} \\ x_{12}(m, p) = x_{\min}(p) + v^{\text{meas}}(p) \left( -t_{\min}(p) + \right. \\ \left. \frac{x_{\max}(m) - x_{\min}(p) + v^{\text{meas}}(p)t_{\min}(p) - vt_{\max}(m)}{v^{\text{meas}}(p) - v} \right) \\ t_{13}(m, p) = \frac{x_{\min}(m) - x_{\min}(p) + v^{\text{meas}}(p)t_{\min}(p) - vt_{\min}(m)}{v^{\text{meas}}(p) - v} \\ x_{13}(m, p) = x_{\min}(p) + v^{\text{meas}}(p) \left( -t_{\min}(p) + \right. \\ \left. \frac{x_{\min}(m) - x_{\min}(p) + v^{\text{meas}}(p)t_{\min}(p) - vt_{\min}(m)}{v^{\text{meas}}(p) - v} \right) \\ t_{14}(m, p) = \frac{x_{\max}(m) - x_{\min}(p) + v^{\text{meas}}(p)t_{\min}(p) - vt_{\max}(m)}{v^{\text{meas}}(p) - w} \\ x_{14}(m, p) = x_{\min}(p) + v^{\text{meas}}(p) \left( -t_{\min}(p) + \right. \\ \left. \frac{x_{\max}(m) - x_{\min}(p) + v^{\text{meas}}(p)t_{\min}(p) - vt_{\max}(m)}{v^{\text{meas}}(p) - w} \right) \\ t_{15}(m, p) = \frac{x_{\min}(m) - x_{\min}(p) + v^{\text{meas}}(p)t_{\min}(p) - vt_{\min}(m)}{v^{\text{meas}}(p) - w} \\ x_{15}(m, p) = x_{\min}(p) + v^{\text{meas}}(p) \left( -t_{\min}(p) + \right. \\ \left. \frac{x_{\min}(m) - x_{\min}(p) + v^{\text{meas}}(p)t_{\min}(p) - vt_{\min}(m)}{v^{\text{meas}}(p) - w} \right) \end{array} \right. \quad (27)$$

*Proof.* Note that  $\forall(k, n) \in [0, k_{\max}] \times [0, n_{\max}]$ ,  $\text{Dom}(M_k) \cap \text{Dom}(\mathbf{M}_{\gamma_n}) = \emptyset$  and that  $\forall(k, n) \in [0, k_{\max}] \times [0, n_{\max}]$ ,  $\text{Dom}(M_k) \cap \text{Dom}(\mathbf{M}_{\beta_n}) = \emptyset$ . Thus, the set of inequality constraints (7) can be written in the case of initial, upstream, downstream

and internal conditions as:

$$\left\{ \begin{array}{l}
 \mathbf{M}_{M_k}(0, x) \geq M_p(0, x) \quad \forall x \in [pX, (p+1)X], \forall (k, p) \in \mathbb{K}^2 \\
 \mathbf{M}_{M_k}(t, \chi) \geq \beta_p(t, \chi) \quad \forall t \in [pT, (p+1)T], \forall (k, p) \in \mathbb{K} \times \mathbb{N} \\
 \mathbf{M}_{M_k}(t, \xi) \geq \gamma_p(t, \xi) \quad \forall t \in [pT, (p+1)T], \forall (k, p) \in \mathbb{K} \times \mathbb{N} \\
 \mathbf{M}_{M_k}(t, x) \geq \mu_m(t, x) \quad \forall t \in [t_{\min}(m), t_{\max}(m)], x = x_{\min}(m) + \\
 \quad v^{\text{meas}}(m)(t - t_{\min}(m)) \forall (k, m) \in \mathbb{K} \times \mathbb{M} \\
 \mathbf{M}_{\gamma_n}(t, \xi) \geq \gamma_p(t, \xi) \quad \forall t \in [pT, (p+1)T], \forall (n, p) \in \mathbb{N}^2 \\
 \mathbf{M}_{\gamma_n}(t, \chi) \geq \beta_p(t, \chi) \quad \forall t \in [pT, (p+1)T], \forall (n, p) \in \mathbb{N}^2 \\
 \mathbf{M}_{\gamma_n}(t, x) \geq \mu_m(t, x) \quad \forall t \in [t_{\min}(m), t_{\max}(m)], x = x_{\min}(m) + \\
 \quad v^{\text{meas}}(m)(t - t_{\min}(m)) \forall (n, m) \in \mathbb{N} \times \mathbb{M} \\
 \mathbf{M}_{\beta_n}(t, \xi) \geq \gamma_p(t, \xi) \quad \forall t \in [pT, (p+1)T], \forall (n, p) \in \mathbb{N}^2 \\
 \mathbf{M}_{\beta_n}(t, \chi) \geq \beta_p(t, \chi) \quad \forall t \in [pT, (p+1)T], \forall (n, p) \in \mathbb{N}^2 \\
 \mathbf{M}_{\beta_n}(t, x) \geq \mu_m(t, x) \quad \forall t \in [t_{\min}(m), t_{\max}(m)], x = x_{\min}(m) + \\
 \quad v^{\text{meas}}(m)(t - t_{\min}(m)) \forall (n, m) \in \mathbb{N} \times \mathbb{M} \\
 \mathbf{M}_{\mu_k}(t, x) \geq \mu_m(t, x) \quad \forall t \in [t_{\min}(m), t_{\max}(m)], x = x_{\min}(m) + \\
 \quad v^{\text{meas}}(m)(t - t_{\min}(m)) \forall (k, m) \in \mathbb{M}^2
 \end{array} \right. \quad (28)$$

The inequalities outlined in Proposition 4.1 result from the above constraints, which can be written as a finite set of inequalities owing the piecewise affine structure of the solutions (13), (12), (14) and (15).

**Fact 4.2. [Linear inequality property]** *The model constraints defined by Proposition 4.1 are linear in the variables  $\rho(1), \rho(2), \dots, \rho(k_{\max}), q_{\text{in}}(1), \dots, q_{\text{in}}(n_{\max}), q_{\text{out}}(1), \dots, q_{\text{out}}(n_{\max}), L_1, \dots, L_{m_{\max}}$  and  $r_1, \dots, r_{m_{\max}}$ .*

While the HJ PDE model constraints (7) ensure that the initial, boundary and internal conditions can all be applied in the strong sense, they do not ensure the continuity of the solution (the solution to the HJ PDE (1) is only lower-semicontinuous in general [4]). In this article, we look for continuous solutions following [22], since they correspond to the physically meaningful solutions. The necessary and sufficient conditions for the continuity of the function  $\mathbf{M}_{\mathbf{c}}(\cdot, \cdot)$  defined by (6) are outlined in Proposition (4.3) below.

**Proposition 4.3. [Continuity constraints]** *Let a set of initial, boundary and internal conditions be defined as in (8), and let the corresponding partial solutions be defined as  $\mathbf{M}_{M_k}(\cdot, \cdot), \mathbf{M}_{\gamma_n}(\cdot, \cdot), \mathbf{M}_{\beta_n}(\cdot, \cdot)$  and  $\mathbf{M}_{\mu_m}(\cdot, \cdot)$ . Let us also assume that the model constraints (7) are satisfied. Let  $\mathbf{M}_p(\cdot, \cdot)$  be defined as  $\mathbf{M}_p(\cdot, \cdot) = \min_{k, n, m | m \neq p}(\mathbf{M}_{M_k}(\cdot, \cdot), \mathbf{M}_{\gamma_n}(\cdot, \cdot), \mathbf{M}_{\beta_n}(\cdot, \cdot), \mathbf{M}_{\mu_m}(\cdot, \cdot))$ . The solution  $\mathbf{M}(\cdot, \cdot)$  to the HJ PDE (5) defined by  $\mathbf{M}(\cdot, \cdot) = \min_{k, n, m}(\mathbf{M}_{M_k}(\cdot, \cdot), \mathbf{M}_{\gamma_n}(\cdot, \cdot), \mathbf{M}_{\beta_n}(\cdot, \cdot), \mathbf{M}_{\mu_m}(\cdot, \cdot))$  is continuous if and only if the following conditions are satisfied:*

$$\begin{aligned}
 \forall p \in \mathbb{M}, \mathbf{M}_p(t_{\min}(p), x_{\min}(p)) &= \mu_p(t_{\min}(p), x_{\min}(p)) & (29) \\
 \left\{ \begin{array}{l}
 \mu_m(t_{\min}(m), x_{\min}(m)) = \min(\mathbf{M}_{M_k}(t_{\min}(m), x_{\min}(m)), \\
 \mathbf{M}_{\gamma_n}(t_{\min}(m), x_{\min}(m)), \mathbf{M}_{\beta_n}(t_{\min}(m), x_{\min}(m)), \\
 \mathbf{M}_{\mu_p}(t_{\min}(m), x_{\min}(m))) \quad \forall k \in \mathbb{K}, \forall n \in \mathbb{N}, \forall (m, p) \in \mathbb{M}^2 \\
 \mu_m(t_{\max}(m), x_{\max}(m)) = \min(\mathbf{M}_{M_k}(t_{\max}(m), x_{\max}(m)), \\
 \mathbf{M}_{\gamma_n}(t_{\max}(m), x_{\max}(m)), \mathbf{M}_{\beta_n}(t_{\max}(m), x_{\max}(m)), \\
 \mathbf{M}_{\mu_p}(t_{\max}(m), x_{\max}(m))) \quad \forall k \in \mathbb{K}, \forall n \in \mathbb{N}, \forall (m, p) \in \mathbb{M}^2
 \end{array} \right. & (30)
 \end{aligned}$$

Furthermore, the inequality constraints (29) can be written as a set of mixed integer linear inequalities involving the continuous variables  $\rho(1), \rho(2), \dots, \rho(k_{\max}), q_{\text{in}}(1), \dots, q_{\text{in}}(n_{\max}), q_{\text{out}}(1), \dots, q_{\text{out}}(n_{\max}), L_1, \dots, L_{m_{\max}}$  and  $r_1, \dots, r_{m_{\max}}$ , as well as auxiliary integer variables.



faults), these constraints have to be feasible. We will use this fact in the following section as a proxy for cyber attack detection.

**4.3. Spoofing cyber attack detection as a mixed integer linear feasibility problem.** Given the model, continuity and data constraints presented above, we consider the following feasibility problem:

$$\begin{aligned} & \text{Find } y \\ & \text{s. t. } \begin{cases} Ay \leq b \\ Cy \leq d \end{cases} \end{aligned} \quad (34)$$

Let us denote by  $\bar{y}$  the actual value of the decision variable corresponding to the actual traffic flow scenario. Note that in experimental situations  $\bar{y}$  cannot be measured, unless one has complete knowledge of the state of the system.

If (34) is infeasible, there is no set of initial, boundary and internal conditions satisfying at the same time the model and data constraints. Thus,  $\bar{y}$  is either violating the model constraints (*i.e.*  $A\bar{y} > b$ ) or the data constraints (*i.e.*  $C\bar{y} > d$ ), or both. The interpretation is as follows:

- If  $\bar{y}$  violates the model constraints, then the actual traffic state function does not follow the HJ PDE (1), which can be caused by modeling errors of the flux function (most probable), or by phenomena that are not modeled by the HJ PDE (1) (less likely).
- If  $\bar{y}$  violates the data constraints, our error model is incorrect. There can be three main reasons for this to happen:
  1. Incorrect error modeling, for instance caused by wrong sensor specifications
  2. Sensor faults (the error model assumes that all sensors are working according to their specifications, *i.e.* non faulty)
  3. Spoofing attacks

If (34) is feasible, there exists a set of initial, boundary and internal conditions compatible both with the traffic flow model and with the observed data. Note that this does not guarantee that no spoofing attack occurs. Indeed, a spoofing attack could occur, but the complete dataset (actual data and spoofed data) would somehow be compatible with the model and the sensor error model. In the remainder of this article, we assume that a spoofing attack is detected whenever (34) is infeasible, though in practice one has to exclude sensor faults or incorrect error modeling before reaching such a conclusion.

**5. Implementation.** We now present an implementation of the spoofing attack detection framework presented earlier on an experimental dataset. The dataset includes fixed sensor data (obtained from inductive loop detectors in the present case) and mobile sensor data.

**5.1. Experimental setup.** As previously, we check the feasibility of (34) as a proxy for cyber attack detection, using the *Mobile Century* [26, 25] dataset. The *Mobile Century* field experiment demonstrated the use of Nokia N-95 cellphones as mobile traffic sensors in February 2008, and was a joint UC-Berkeley/Nokia project.

For the numerical applications, a spatial domain of 3.858 km is considered, located between the PeMS [27] VDSs (*vehicle detection stations*) 400536 and 400284

on the Highway I - 880 N around Hayward, California. The data used in this implementation was generated on February 8<sup>th</sup>, 2008, between times 18 : 30 and 18 : 55 (local time). In our scenario, we consider inflow and outflow data  $q_{in}^{\text{measured}}(\cdot)$  and  $q_{out}^{\text{measured}}(\cdot)$  generated by the above PeMS stations, *i.e.* we do not assume to know any initial density data. We also consider internal condition data (*i.e.* probe vehicle data), either real (*i.e.* extracted from the *Mobile Century* dataset) or spoofed (drawn randomly according to a specific distribution). The layout of the spatial domain is illustrated in Figure 2.

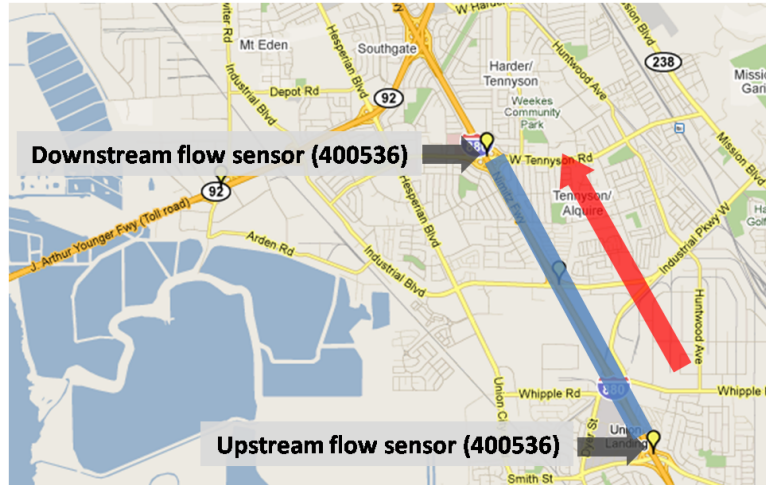


FIGURE 2. **Spatial domain considered for the numerical implementation.** The upstream and downstream PeMS stations are delimiting a 3.858 km spatial domain, outlined by a solid line. The direction of traffic flow is represented by an arrow.

For all subsequent applications, the data constraints are chosen and assumed to be linear:  $(1-e)q_{in/out}^{\text{measured}}(n) \leq q_{in/out}(n) \leq (1+e)q_{in/out}^{\text{measured}}(n) \quad \forall n \in [0, n_{\max}]$ , where  $e = 0.01 = 1\%$  is chosen the worst-case relative error of the flow sensors.

We divided the spatial domain into four segments of equal distance  $X=965$  m. We also set  $T=30$  s as the aggregation time for the flow data ( $T$  is determined by the granularity of PeMS data). All MILPs have been implemented using IBM Ilog Cplex working on a Macbook operating MacOS X. The problems described in this article are tractable: they typically involve hundreds of variables and thousands of constraints, and are solved in a few tens seconds.

**5.2. Cyber attack detection example.** Our objective is to show the effects of a spoofing attack on traffic flow estimates using mixed boundary flow and probe vehicle data. For this specific application the objective function is chosen as the total number of vehicles at initial time, defined by  $\sum_{i=0}^{k_{\max}} \rho(i)$ , though we are mostly interested in the feasibility of the model and data constraints, which will act as a proxy for detecting fake data injection. We consider 20 blocks of upstream (9) and downstream (10) boundary conditions as well as 6 blocks of (real) internal (11) conditions.

As no spoofed data is injected, (34) is feasible, and the traffic density maps corresponding to the minimum and maximum values of the objective function are shown in Figure 3 below.

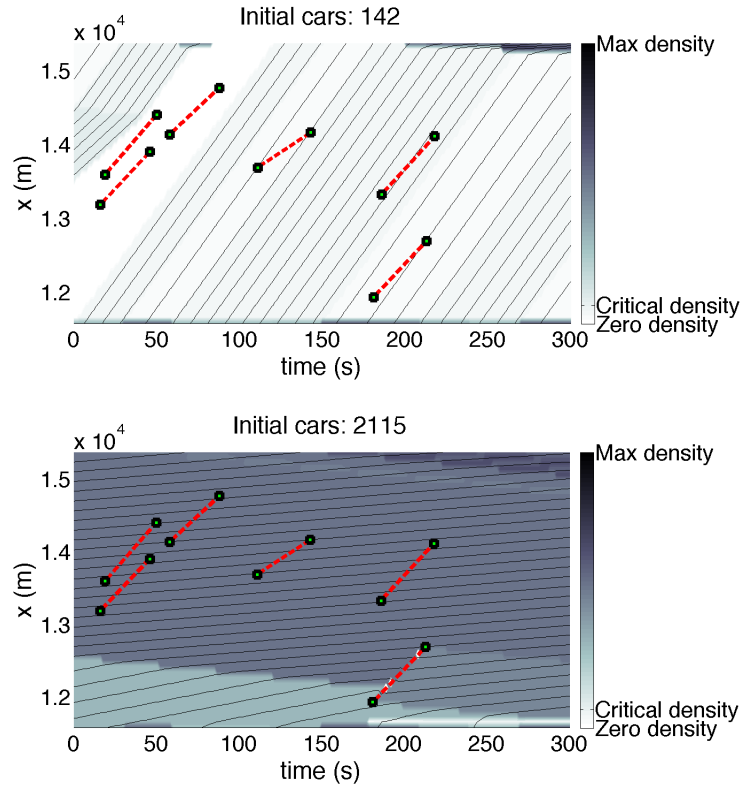


FIGURE 3. **Scenarios corresponding to the minimum and maximum number of vehicles (no spoofing attack).** In all subfigures, we compute the scenario for which the initial number of vehicles is the largest (or the smallest), given the boundary data as well as probe data (dashed segments) **Top:** minimized number of vehicles. **Bottom:** maximized number of vehicles.

We now simulate the effects of a spoofing attack on the traffic estimates, as well as its detection by the proposed scheme. For this, we progressively incorporate spoofed probe data in the problem and check the solution to (34). An attack is detected when (34) becomes infeasible.

For our specific scenario, infeasibility occurred after we added only 3 fake internal conditions when the former were drawn from a normal distribution centered around 15 mph, with a standard deviation of 1.25 mph. Note that average speed reported by the vehicles was around 40 mph, with a standard deviation of 10 mph. Since the traffic speed was higher than the velocity of the fake internal conditions, these additions tend to increase the estimated minimal possible density of vehicles on the highway, as illustrated in Figure 4. In contrast, adding fake speed data that is closer to the current traffic conditions is more likely to go undetected, as illustrated

IC velocity range (mph)	0-10	10-20	20-30	30-40
# IC for infeasibility (set 1)	1	1	1	1
# IC for infeasibility (set 2)	1	1	2	4
# IC for infeasibility (set 3)	1	1	2	3

TABLE 1. **Number of internal conditions required for infeasibility of (34) on different scenarios.** We consider the same problem as previously, with 6 blocks of real internal conditions, and randomly generate sets of internal conditions associated with some speed range. The faked internal conditions from the corresponding sets are then added in order into (34), until the problem becomes infeasible. Low numbers mean that an attack is detected almost immediately, while large numbers indicate that some amount of faked data can go unnoticed by the model/data consistency check.

with the scenario illustrated in Figure 4, bottom. In this specific scenario, six fake internal conditions were randomly chosen with a mean value of 35 mph and a standard deviation of 1.25 mph. These fake internal conditions have a stronger effect on the estimation of the minimal number of vehicles than in the previous case, and go undetected since they do not alter the velocity profile too significantly. Hence, the best strategy for an attacker is not necessarily to inject fake data that is too far away from the current traffic condition.

The mixed integer linear constraints arising from the model and from the data define a feasible set in which the real coefficients of the initial, boundary and internal conditions lie. Adding spoofing data will generate additional inequality constraints, which will reduce the size of the feasible set. Hence, spoofing cyber attacks can narrow down the estimates to a specific point of the feasible set, giving artificial confidence in the (wrong) estimates generated by the system.

**5.3. Effects of average speed and vehicle distribution on cyber attack detection.** We now illustrate on a specific example the ability of the algorithm to detect a cyber attack resulting from a faked internal condition that would result in a model violation. In this specific example, we consider 20 blocks of upstream (9) and downstream (10) boundary conditions as well as 6 blocks of (real) internal (11) conditions. We add a single internal condition associated with a very low speed (compared to the speed estimated by the model in the area of influence of this internal condition). As expected, problem (34) becomes infeasible with this new internal condition. This example is illustrated in Figure 5.

We now illustrate the effects of the average velocity associated with the faked internal conditions on cyber attack detection. As before, we consider 20 blocks of upstream (9) and downstream (10) boundary conditions as well as 6 blocks of (real) internal (11) conditions. We then generate 12 different sets of internal conditions associated with different speed ranges of internal conditions (3 sets per speed range), and progressively add these internal conditions until problem (34) becomes infeasible. The results are summarized in table 1.

In this specific scenario, the vehicle speed range on the highway was between 30-50 mph. Hence, very low speeds are very likely to cause an infeasibility of the model and data constraints, and indeed an attacker sending such faked internal conditions

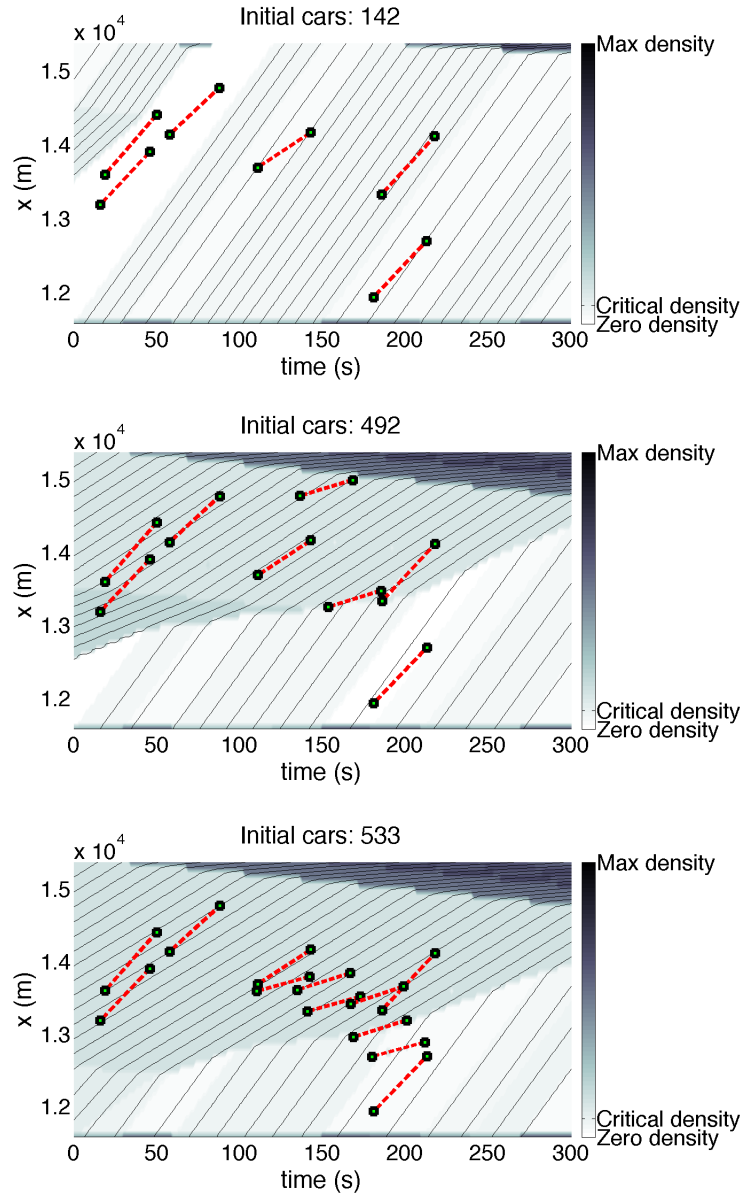


FIGURE 4. Scenarios corresponding to the computed minimum number of vehicles with spoofing attacks. The scenario is identical to 3 with the addition of spoofed data. Whenever spoofed data is considered, we consider the scenario perturbed by the spoofed data for which an additional piece of spoofed data leads to the detection of the attack by the proposed scheme. **Top:** minimized number of vehicles with no fake internal condition. **Center:** minimized number of vehicles with two additional fake internal conditions chosen randomly with a mean value of 15 mph and a standard deviation of 1.25 mph. **Bottom:** minimized number of vehicles with six additional fake internal conditions chosen randomly with a mean value of 35 mph and a standard deviation of 1.25 mph.

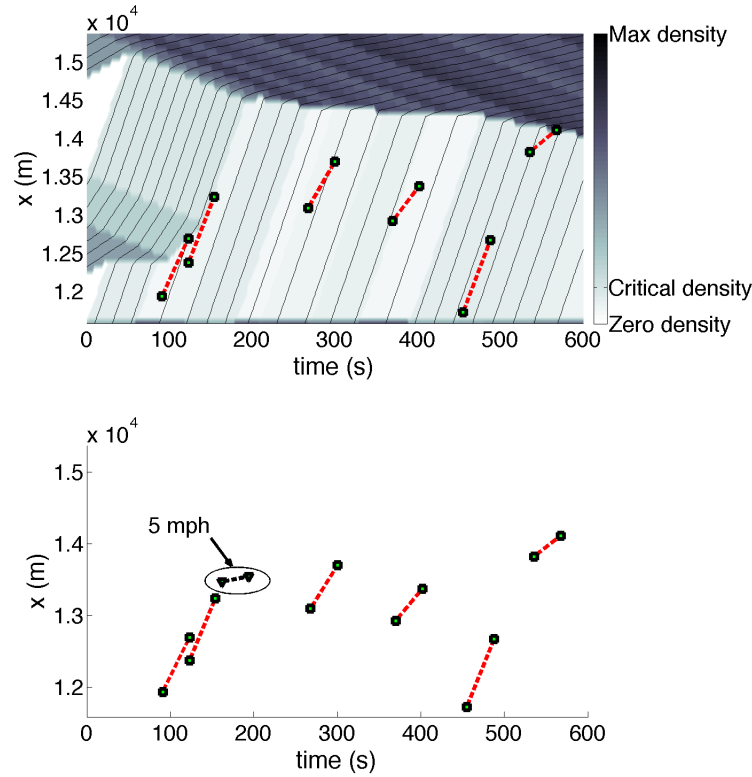


FIGURE 5. **Example of cyber attack detection.** This scenario shows how a single internal condition associated with an unreasonable velocity (compared with the model prediction) can result in an infeasibility of problem (34). **Top:** maximized number of vehicles with no faked internal condition (corresponding to lowest possible average velocity). **Bottom:** configuration of the internal conditions resulting in an infeasibility of (34). The faked internal condition is highlighted in black, and is corresponding to a speed that is much slower than the worst-case speed forecasted by the model in this area.

in the system would be detected immediately. Of course, faked internal conditions corresponding to speeds that are consistent with the average speed of traffic are more likely to go undetected (as in the speed range 30 – 40 mph in table 1), but not always, as illustrated by the first line of this table. In this specific cases, the spatio-temporal locations of the internal conditions caused an infeasibility of (34).

**6. Conclusion.** In this article, we introduce a new numerical scheme for detecting data-spoofing cyber attacks on systems modeled by first order scalar conservation laws, such as the highway transportation network. We first present an equivalent formulation of the problem based on a Hamilton-Jacobi equation. Using a semi-analytical expression of the solutions to the Hamilton-Jacobi equation, we formulate the problem of checking the consistency of the data with respect to the model as a Mixed Integer Linear Program (MILP). The method does not require any approximation or Monte-Carlo simulations to operate, and is tractable. We illustrate the performance of the method on an experimental probe dataset.

Future work will be dedicated to the generalization of the method to allow model uncertainty. In general, the corresponding problem becomes nonconvex feasibility program, which might still be tractable through relaxations or approximations. Another important direction is the study of spoofing cyber attacks on transportation networks, to take into account the coupling effect of junctions and possibly detect such attacks earlier. Other applications of the framework presented in this article are possible, such as the real time assessment of the vulnerability of a system to spoofing attacks, or sensor fault detection.

## REFERENCES

- [1] S. Amin, A. Cardenas and S. Sastry, *Safe and secure networked control systems under denial-of-service attacks*, in “Proceedings of the 12th International Conference on Hybrid Systems: Computation and Control,” Springer-Verlag, (2009), 31–45.
- [2] S. Amin, X. Litrico, S. Sastry and A. Bayen, *Stealthy deception attacks on water scada systems*, In “Proceedings of the 13th ACM International Conference on Hybrid Systems: Computation and Control,” ACM, (2010),161–170.
- [3] J.-P. Aubin, “Viability Theory,” Systems and Control: Foundations and Applications, Birkhäuser, Boston, MA, 1991.
- [4] J.-P. Aubin, A. M. Bayen and P. Saint-Pierre, *Dirichlet problems for some Hamilton-Jacobi equations with inequality constraints*, SIAM Journal on Control and Optimization, **47** (2008), 2348–2380.
- [5] M. Bardi and I. Capuzzo-Dolcetta, “Optimal Control and Viscosity Solutions of Hamilton-Jacobi-Bellman Equations,” Birkhäuser, Boston, MA, 1997.
- [6] E. N. Barron and R. Jensen, *Semicontinuous viscosity solutions for Hamilton-Jacobi equations with convex Hamiltonians*, Communications in Partial Differential Equations, **15** (1990), 1713–1742.
- [7] E. S. Canepa and C. G. Claudel, *Exact solutions to traffic density estimation problems involving the Lighthill-Whitman-Richards traffic flow model using Mixed Integer Linear Programming*, In “Proceedings of the 15th International IEEE Conference on Intelligent Transportation Systems”, (2012), 832–839.
- [8] P. D. Christofides, “Nonlinear and Robust Control of Partial Differential Equation Systems: Methods and Applications to Transport-Reaction Processes,” Birkhäuser, Boston, MA, 2001.
- [9] C. G. Claudel and A. M. Bayen, *Lax-Hopf based incorporation of internal boundary conditions into Hamilton-Jacobi equation. Part I: Theory*, IEEE Transactions on Automatic Control, **55** (2010), 1142–1157.
- [10] C. G. Claudel and A. M. Bayen, *Lax-Hopf based incorporation of internal boundary conditions into Hamilton-Jacobi equation. Part II: Computational methods*, IEEE Transactions on Automatic Control, **55** (2010), 1158–1174.
- [11] C. G. Claudel and A. M. Bayen, *Convex formulations of data assimilation problems for a class of Hamilton-Jacobi equations*, SIAM Journal on Control and Optimization, **49** (2011), 383–402.
- [12] M. G. Crandall and P.-L. Lions, *Viscosity solutions of Hamilton-Jacobi equations*, Transactions of the American Mathematical Society, **277** (1983), 1–42.
- [13] C. Daganzo, *The cell transmission model: a dynamic representation of highway traffic consistent with the hydrodynamic theory*, Transportation Research, **28B** (1994), 269–287.
- [14] C. F. Daganzo, *A variational formulation of kinematic waves: basic theory and complex boundary conditions*, Transportation Research B, **39B** (2005), 187–196.
- [15] C. F. Daganzo, *On the variational theory of traffic flow: well-posedness, duality and applications*, Networks and Heterogeneous Media, **1** (2006), 601–619.
- [16] H. Frankowska, *Lower semicontinuous solutions of Hamilton-Jacobi-Bellman equations*, SIAM Journal of Control and Optimization, **31** (1993), 257–272.
- [17] J. C. Herrera, D. B. Work, R. Herring, X. J. Ban, Q. Jacobson and A. M. Bayen, *Evaluation of traffic data obtained via GPS-enabled mobile phones: The Mobile Century field experiment*, Transportation Research Part C: Emerging Technologies, **18** (2010), 568–583.
- [18] B. Hoh, M. Gruteser, R. Herring, J. Ban, D. Work, J. C. Herrera, A. M. Bayen, M. Annavaram and Q. Jacobson, *Virtual trip lines for distributed privacy-preserving traffic monitoring*, in

- “Proceedings of the 6th International Conference on Mobile Systems, Applications, and Services,” ACM, (2008), 15–28.
- [19] M. Krstic and A. Smyshlyaev, *Backstepping boundary control for first-order hyperbolic pdes and application to systems with actuator and sensor delays*, Systems & Control Letters, **57** (2008), 750–758.
- [20] P. E. Mazare, A. Dehwah, C. G. Claudel and A. M. Bayen, *Analytical and grid-free solutions to the lighthill-whitham-richards traffic flow model*, Transportation Research Part B: Methodological, **45** (2011), 1727–1748.
- [21] K. Moskowitz, *Discussion of ‘freeway level of service as influenced by volume and capacity characteristics’ by D.R. Drew and C. J. Keese*, Highway Research Record, **99** (1965), 43–44.
- [22] G. F. Newell, *A simplified theory of kinematic waves in highway traffic, Part (I), (II) and (III)*. Transportation Research B, **27B** (1993), 281–313.
- [23] R. C. Smith and M. A. Demetriou, “Research Directions in Distributed Parameter Systems,” SIAM, Philadelphia, PA, 2000.
- [24] I. S. Strub and A. M. Bayen, *Weak formulation of boundary conditions for scalar conservation laws*, International Journal of Robust and Nonlinear Control, **16** (2006), 733–748.
- [25] D. Work, S. Blandin, O. Tossavainen, B. Piccoli and A. Bayen, *A distributed highway velocity model for traffic state reconstruction*, Applied Research Mathematics eXpress (ARMX), **1** (2010), 1–35.
- [26] <http://traffic.berkeley.edu/>.
- [27] <http://pems.dot.ca.gov>.

Received September 2012; revised March 2013.

E-mail address: [edward.canepa@kaust.edu.sa](mailto:edward.canepa@kaust.edu.sa)

E-mail address: [bayen@berkeley.edu](mailto:bayen@berkeley.edu)

E-mail address: [christian.claudel@kaust.edu.sa](mailto:christian.claudel@kaust.edu.sa)